



ORIGINAL ARTICLE

Ultrastructure of the archigregarine *Selenidium vivax* (Apicomplexa) – A dynamic parasite of sipunculid worms (host: *Phascolosoma agassizii*)

BRIAN S. LEANDER

Canadian Institute for Advanced Research, Program in Evolutionary Biology, Departments of Zoology and Botany, University of British Columbia, Vancouver, BC, V6T 1Z4, Canada

Abstract

Selenidium vivax is a large and unusual unicellular parasite that inhabits the intestinal lumen of the dotted peanut worm, *Phascolosoma agassizii*. Molecular phylogenies suggest that this archigregarine lineage diverges near the nexus of the apicomplexan radiation and could shed light on to the early evolution of parasitism within the group. The behaviour and ultrastructure of the trophozoites were described using digital videography and scanning and transmission electron microscopy. The trophozoites were extremely flat and capable of dynamic cellular deformations. An intimate association between a superficial layer of mitochondria and longitudinal clusters of subpellicular microtubules formed a distinct functional configuration that helped explain the mechanism behind the cellular motility. Although inconclusive, the presence of small mitochondria-like profiles and narrow connections between larger mitochondrial profiles suggested that an expansive mitochondrial reticulum might surround the trophozoites. The nucleus was highly convoluted and gave rise to blebs of different sizes. The nuclear blebs were connected to the nucleus proper and surrounded by one cisterna of endoplasmic reticulum, giving the impression of four membrane-bound organelles that were misleadingly reminiscent of apicoplasts. The novel attachment apparatus consisted of a transverse ridge, a linear arrangement of pores that contained thread-like structures and a network of dense bodies and endoplasmic reticulum.

Key words: *Apicomplexa*, *archigregarine*, *evolution*, *parasite*, *Selenidium*, *sipunculid*, *ultrastructure*

Introduction

Archigregarines are an ill-defined group of apicomplexans that are parasitic of intestinal systems in a wide range of marine invertebrates, especially polychaetes. Like gregarines in general, the haploid lifecycle of archigregarines consists of relatively large feeding cells, the “trophozoites”, that inhabit extra-cellular spaces within the animal host and pair up with one another in a process known as “syzygy”, which marks the onset of sexual reproduction. A gametocyst forms around these pairings (i.e. the “gamonts”) within which hundreds of gametes are formed by multiple rounds of mitosis. Gametes derived from different gamonts fuse to form zygotes (the fleeting diploid stage), which develop into robust oocysts. (Note that “oocyst” and “sporocyst” are synonymous in the gregarine literature. These

terms, however, have very different meanings in the coccidian literature.) Meiosis within each oocyst usually produces four banana-shaped sporozoites. However, sporozoite numbers ranging from six to 16 have also been reported in some archigregarines (Grassé 1953; Levine 1971). In eugregarines, additional rounds of mitosis can produce more sporozoites per oocyst. In the case of archigregarines and intestinal eugregarines (e.g. *Lecudina*, *Lankesteria* and *Gregarina*), the oocysts, via the gametocysts, leave an infected host with the faeces and become widely distributed in the environment only to be orally ingested by other hosts living in the same environment.

Once ingested by the new host, the sporozoites excyst and infect the host intestinal epithelium. It has been suggested that some archigregarines undergo “merogony” (Levine 1971), which is the

Correspondence: B. Leander, #3529-6270 University Blvd, Departments of Botany and Zoology, University of British Columbia, Vancouver, BC, V6T 1Z4, Canada. E-mail: bleander@interchange.ubc.ca

Published in collaboration with the University of Bergen and the Institute of Marine Research, Norway, and the Marine Biological Laboratory, University of Copenhagen, Denmark

(Accepted 29 March 2006; Printed 24 July 2006)

ISSN 1745-1000 print/ISSN 1745-1019 online © 2006 Taylor & Francis

DOI: 10.1080/17451000600724395

asexual multiplication of either sporozoites or trophozoites. The absence of merogony in most species has been used to exclude them from the archigregarines *sensu stricto* and has resulted in the disruption of otherwise highly cohesive genera (e.g. *Selenidium* versus *Selenidioides*) (Levine 1971). Because observing merogony is not straightforward and “demonstrating an absence” is difficult, I have chosen not to follow this taxonomic scheme and instead refer to members of *Selenidium* as archigregarines *sensu lato*, which is consistent with other workers in the field (Schrével 1971a,b; Théodoridès 1984; Gunderson & Small 1986; Kuvardina & Simdyanov 2002).

An unambiguous synapomorphy for the archigregarines has yet to be identified, probably because members of the group have retained several features that appear to be plesiomorphic for the Apicomplexa as a whole. Unlike in eugregarines, where trophozoite morphology and behaviour are significantly different from the sporozoites from which they develop, the intracellular sporozoite and extracellular trophozoite stages in archigregarines are often remarkably similar but differ in size (Schrével 1971a,b). For instance, both stages are often spindle-shaped, capable of undulating movements and have an apical complex (Ray 1930; Schrével 1968, 1970; Dyson et al. 1993, 1994; Kuvardina & Simdyanov 2002). The trophozoites appear to use the apical complex for feeding by myzocytosis (the process whereby a predatory cell pierces the wall of a prey cell or host cell and withdraws the cytoplasmic contents into a food vacuole) (Schrével 1968). This mode of feeding is also present in the nearest free-living relatives of the parasitic apicomplexans, namely colpodellids (Myl'nikov 1991, 2000; Simpson & Patterson 1996; Kuvardina et al. 2002; Leander et al. 2003b; Cavalier-Smith & Chao 2004). Moreover, unlike in eugregarines, the cell surface of archigregarine trophozoites has relatively few folds (e.g. <60 longitudinal striations). Archigregarines are also confined to marine environments and the intestinal tracts of their invertebrate hosts, and like all other gregarines and many coccidians, they complete their lifecycle within a single host. For all of the above reasons, several authors have speculated that archigregarines might form the paraphyletic stem group from which all other apicomplexans have evolved (Grassé 1953; Théodoridès 1984; Vivier & Desportes 1990; Cox 1994; Leander & Keeling 2003; Leander et al. 2006). Although inconclusive, molecular phylogenetic analyses have so far been consistent with this inference (Leander et al. 2003a, 2006; Cavalier-Smith & Chao 2004).

Nonetheless, many archigregarine species appear to be highly derived along independent evolutionary

trajectories (Ray 1930; Schrével 1970; Kuvardina & Simdyanov 2002; Leander et al. 2003a). Here we present one such example by characterizing the ultrastructure of an archigregarine that inhabits the intestinal tracts of the sipunculid *Phascolosoma agassizii*, namely *Selenidium vivax*. This archigregarine was first described in 1986, but no micrographs of any kind were presented at that time (Gunderson & Small 1986). Subsequently, this species was studied with scanning electron microscopy (SEM) and molecular phylogenetics using the small subunit rRNA marker (Leander et al. 2003a). Molecular phylogenetic analyses demonstrated that *S. vivax* is a divergent lineage that branches near the nexus of the apicomplexan radiation. These data, combined with the highly unusual morphological features found in this species, led me to further examine its ultrastructural characteristics using real-time digital videography, SEM and transmission electron microscopy (TEM).

Material and methods

Collection of organisms

Forty individuals of the sipunculid *Phascolosoma agassizii* Keferstein, 1967 were collected at low tide (0.2–0.3 m above the mean low tide) from the rocky pools of Grappler Inlet near the Bamfield Marine Sciences Centre, Vancouver Island, Canada in June 2003. Trophozoites that conformed exactly to the species description of *S. vivax* were isolated from the convoluted intestines of five different worms (Gunderson & Small 1986).

Light microscopy

Trophozoites were observed and micromanipulated with a Leica MZ6 stereomicroscope and a Leica DMIL inverted microscope. Micropipetted trophozoites were washed with filtered seawater and placed on a glass specimen slide. Digital movies and differential interference contrast images of individual trophozoites were produced with a Zeiss Axiovert inverted microscope connected to a PixeLink Megapixel colour camera.

SEM

Trophozoites were released into seawater by teasing apart the intestine of the sipunculids with fine-tipped forceps. Approximately 20 parasites were removed from the remaining gut material by micromanipulation and washed twice in filtered seawater. Individual trophozoites were deposited directly into the threaded hole of a Swinnex filter holder, containing a 5 µm polycarbonate membrane filter (Coring

Separations Division, Acton, MA, USA) submerged in 10 ml of seawater within a small canister (2 cm diameter and 3.5 cm tall). Whatman filter paper was mounted on the inside base of a beaker (4 cm diameter and 5 cm tall) and saturated with 4% OsO₄. Placing the beaker over the canister fixed the parasites with OsO₄ vapours. After 30 min of vapour fixation, six drops of 4% OsO₄ were added directly to the seawater and the parasites were fixed for an additional 30 min. A 10 ml syringe filled with 30% ethanol was screwed to the Swinnex filter holder and the entire apparatus was removed from the canister containing seawater and fixative. The trophozoites were dehydrated with a graded series of ethyl alcohol and critical-point dried with CO₂. Filters were mounted on stubs, sputter coated with gold, and viewed under a Hitachi S4700 SEM. Some SEM micrographs were created from montages of three individual images of the same cell and illustrated on black backgrounds using Adobe Photoshop 6.0 (Adobe Systems, San Jose, CA, USA).

TEM

Approximately 25 trophozoites were concentrated in an Eppendorf tube by micropipetting and slow centrifugation. The small pellet of parasites was pre-fixed with 2% (v/v) glutaraldehyde at 4°C for 30 min in filtered seawater. Trophozoites were washed twice in filtered seawater before post-fixation in 1% (w/v) OsO₄ for 30 min at room temperature. Cells were dehydrated through a graded series of ethanol, infiltrated with acetone–resin mixtures (pure acetone, 3:1, 1:1, 1:3, pure resin) and embedded in pure resin. The block was polymerized at 60°C and sectioned with a diamond knife on a Leica Ultracut UltraMicrotome. Thin sections (70–85 µm) were post-stained with uranyl acetate and lead citrate and viewed under a Hitachi H7600 TEM.

Results

Cell shape and motility

The extracellular trophozoites of *S. vivax* were highly active and capable of extreme cellular deformations (Figure 1). The general shape of the trophozoites is best described as tape-like and approximately 120–500 µm in length, 15–80 µm in width and 2–15 µm in depth. The cell shape, however, was never static. Each trophozoite was capable of folding on itself (Figure 1D–G, T–Z) and could twist, stretch and contract different cell regions independently of one another (Figure 1H–T). This behaviour is perhaps best described as “metaboloid movement” because it is reminiscent of

metabolism in some euglenids. The anterior end of the trophozoites was also plastic and had a wide range of morphologies, including edge-like (Figures 1H, I, O, 2A, C), pointed (Figure 1G, N, S) and multi-digitated (Figure 1V, W). The posterior end tapered to a blunt point in relatively extended trophozoites and could be more rounded in contracted trophozoites (Figures 1, 2A–D). Peristaltic waves were also observed and usually passed from the posterior end to the anterior end of the cell (Figure 2A, B).

Cell surface and cytoskeleton

Crests in the lateral margin of the cell were associated with transient longitudinal striations in the cell surface that were reminiscent of the body folds of most other archigregarines (Figure 2A–D). The trophozoites of *S. vivax* also had transverse striations distributed over the surface of contracted cell regions (Figures 2C, D, 3A–E). The transverse striations had three distinct but related morphologies, including: (1) transverse series of small longitudinal ridges aligned in parallel (Figure 3C), (2) transverse striations supported basally by small longitudinal ridges (Figure 3D) and (3) smooth transverse striations that terminate with tapered ends (Figure 3E). TEM confirmed that the transverse striations were a series of organized folds (wrinkles) in the plasma membrane and subtending inner membrane complex (Figure 3F). The inner membrane complex or pellicle was comprised of three layers and was consistent in structure to that found in other apicomplexans (Figure 3I). The internal structure of the transverse folds was devoid of microtubules. However, the bases of the transverse folds were subtended by dense bundles of microtubules that were oriented along the longitudinal axis of the cell (i.e. perpendicular to the transverse folds) (Figure 3F). Weakly associated bundles of microtubules were evident in transverse sections through the cell surface, which corresponded to the transient longitudinal striations on the cell surface (Figure 3G–J). Micropores were not observed, except near the anterior attachment apparatus (see below).

Mitochondria and multiple membrane-bound organelles

Longitudinal sections through the trophozoites demonstrated a complex cytoplasm consisting of vacuoles, mitochondria, paraglycogen granules (= amylopectin), Golgi bodies and several types of multiple membrane-bound organelle (Figures 4A–F, 5A–E). The mitochondria were localized to the most superficial regions of the cytoplasm (Figure 4A–F) and were not observed in the deeper regions

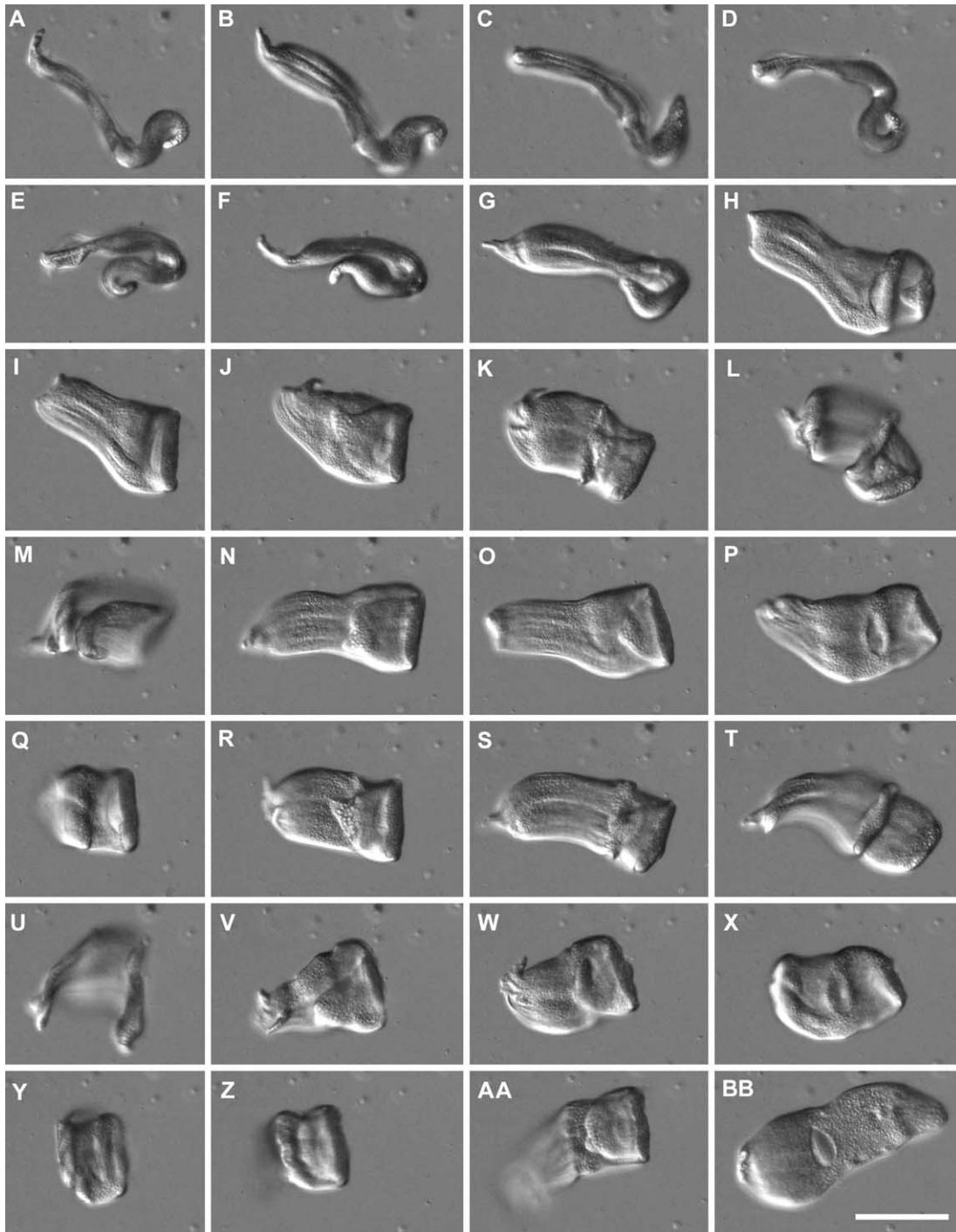


Figure 1. A trophozoite of *Selenidium vivax* isolated from the intestines of the sipunculid, *Phascolosoma agassizii*. (A–BB) A time series of differential interference contrast micrographs (1 frame s^{-1}) showing the general cell shapes and convoluted wriggling movements of trophozoites; the anterior end of the cell is oriented to the left. The trophozoites had relatively large tape-like cell shapes that actively changed in conformation by twisting, folding, shrinking and expanding the cell volume (bar = $30 \mu\text{m}$).

of the cytoplasm. It was not definitively determined whether the independent mitochondrial profiles were linked together within a large reticulum or constituted a population of disconnected organelles. Nonetheless, a dense layer of mitochondria was always present immediately beneath the longitudinal bundles of pellicular microtubules (Figures 4,

5A). The region between the mitochondrial profiles and the pellicular microtubules contained small circular profiles ($\sim 0.1 \mu\text{m}$ in diameter) that were otherwise similar in structure to the mitochondria (Figure 5A).

The mitochondria had tubular cristae and often contained a ring-shaped inclusion consisting of a

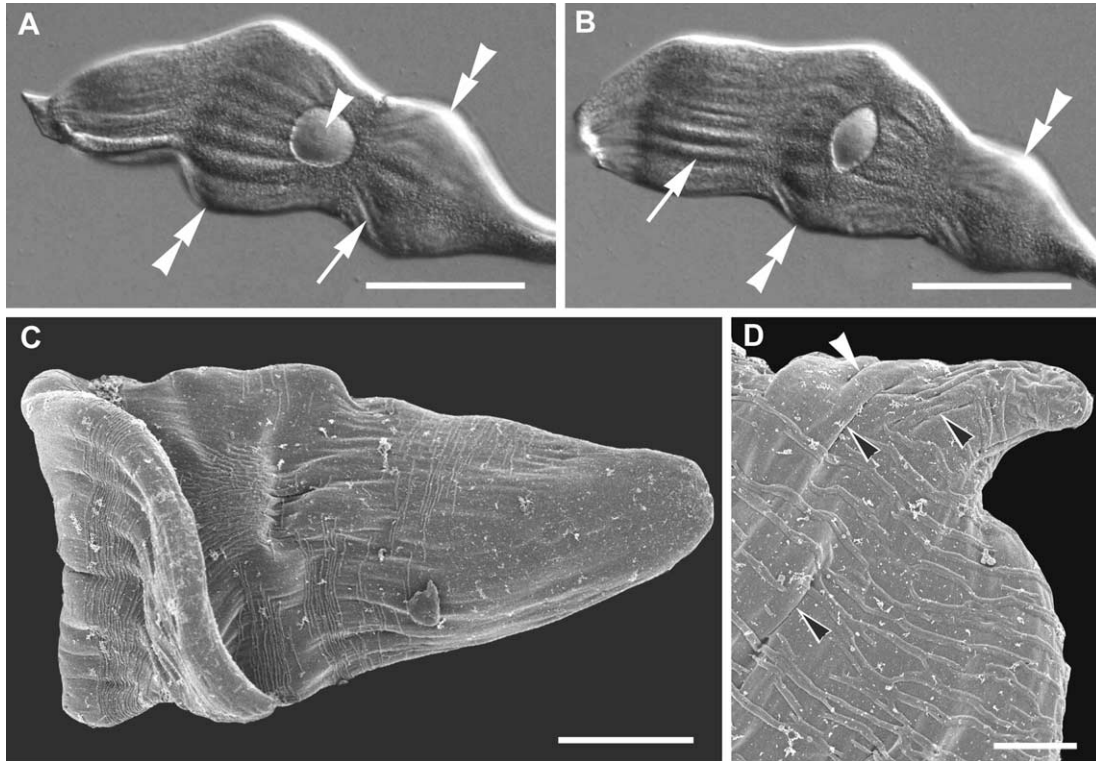


Figure 2. Light and electron micrographs of *Selenidium vivax* showing general trophozoite characteristics. (A, B) Differential interference contrast light micrographs showing the generation and progression of peristaltic waves moving from the posterior end to the anterior end of the cell. As crests in the lateral margin (double arrowheads) moved anteriorly (the left-hand side of the images) and passed over the nucleus, the nuclear shape changed from circular to ovoid; the nucleolus did not change shape (arrowhead). Longitudinal striations in the cell surface (arrows) reflected an underlying mechanism for the generation and co-ordination of the metaboloid movements (bars = 50 μm). (C) Scanning electron micrograph (SEM) of a folded trophozoite; the anterior end is oriented to the left and towards the viewer (bar = 5 μm). (D) SEM of the posterior tip of a trophozoite showing a folded cell surface (black and white arrows) in a twisted conformation (bar = 5 μm).

double membrane (Figure 5B, C). This ring-shaped inclusion was occasionally pressed against the inner mitochondrial membrane of smaller profiles, giving the appearance of a four membrane-bound organelle (Figure 5C). Less common structures consisted of several concentrically nested membranes (Figure 5D–E). Bundles of two or three microtubules were occasionally observed deep within the cytoplasm (data not shown).

Nucleus

The large nucleus of *S. vivax* was positioned in the centre of trophozoites, bulging from the relatively flat surfaces (Figure 6A), and possessed a conspicuous nucleolus that was consistent in size with previous reports (Gunderson & Small 1986). The nucleus changed shape from spherical to ovoid as the waves of contraction passed over the centre of the trophozoites; the nucleolus did not change shape (Figure 2A, B). The ultrastructure of the nucleus consisted of homogeneous euchromatin, a darkly stained nucleolus and a vesicular layer immediately inside the nuclear envelope (Figure 6A–C). The margin of the nuclear envelope was often highly

convoluted, giving rise to finger-like extensions and nuclear blebs of various sizes (Figure 6B–D). The nuclear blebs were frequently observed attached to the nucleus proper by a thin stalk (Figure 6D). One cisterna of endoplasmic reticulum surrounded the nuclear envelope, including the nuclear blebs. The two membranes of the nuclear envelope combined with the cisterna of endoplasmic reticulum around the nuclear blebs gave the appearance of four membrane-bound organelles near the nucleus (Figure 6C–E).

Attachment apparatus/mucron

The most stable configuration of the anterior end of trophozoites took the form of a straight edge (Figures 2C, 7A). The edge consisted of a continuous transverse ridge that spanned the entire width of the cell and was adjacent to a linear series of pores (Figure 7A, B). Discontinuous ridges delimited the pores on the opposite side of the transverse ridge. Vermiform-shaped structures emerged from some of the pore openings (Figure 7A, C). The cytoplasm near the anterior end contained a large accumulation of dense bodies and an elaborate system of endo-

plasmic reticulum (Figure 7D, E). This region of the cytoplasm also contained an unidentified linear structure consisting of the following components: a continuous thread flanked on one side (left in Figure 7F) by a putative membrane and flanked on the

other side (right in Figure 7F) by a linear row of small granules. A cluster of seven small granules was also evident on the opposite side (left in Figure 7F) of the thread (Figure 7D, F). The three-dimensional nature of this structure was unclear. Although a few

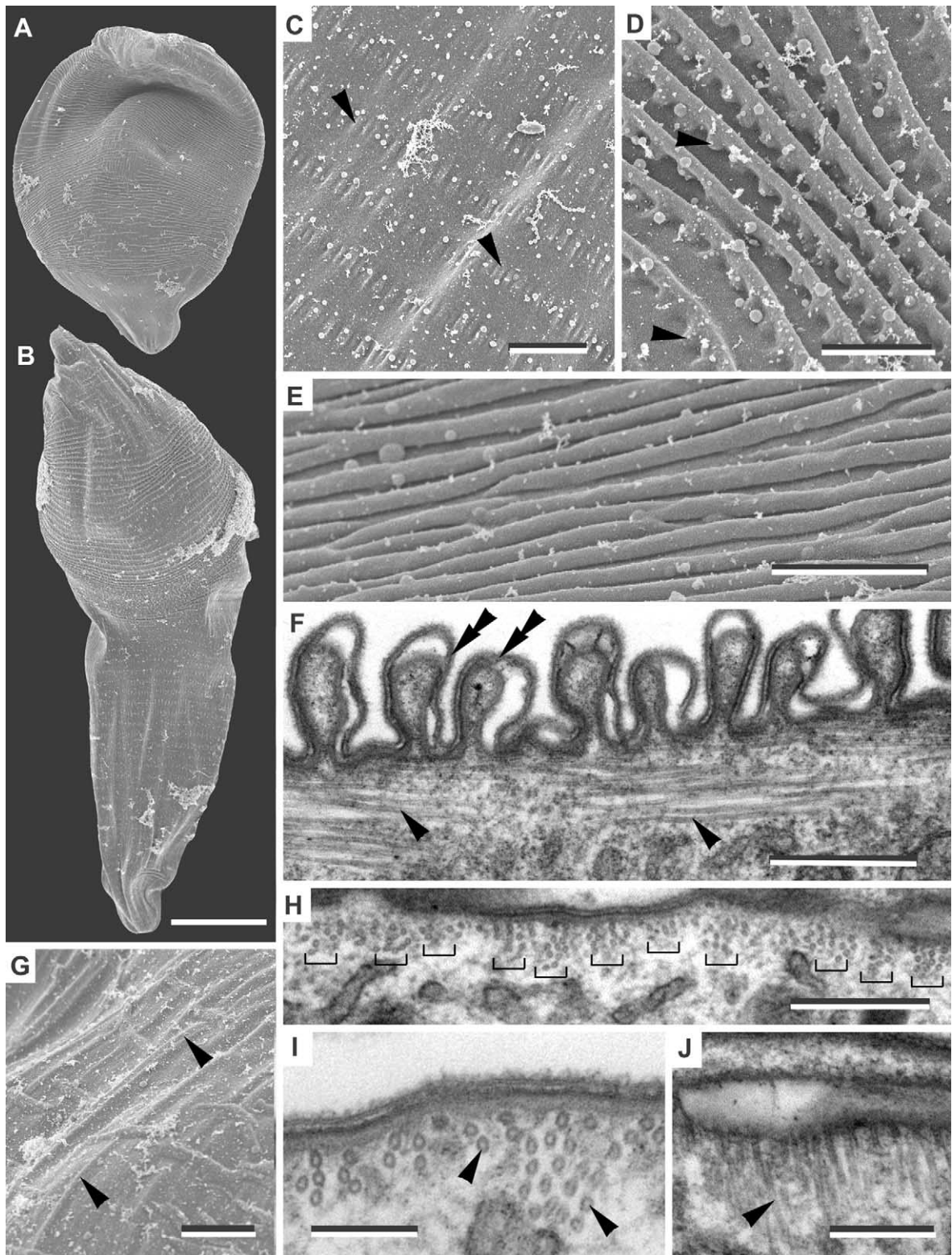


Figure 3 (Continued)

microtubules were observed near the bases of some pores, no evidence of a conoid was observed (Figure 7H). The pores of the attachment apparatus pierced the plasma membrane and the inner membrane complex (Figure 7G, H).

Discussion

The large, flattened cell shape of *S. vivax* has also been observed in a few other gregarine parasites that infect sipunculid worms, namely *S. folium*, *S. orientale*, *S. franciana*, *S. stellatum*, *S. cantoui* and *Exoschizon siphonosomae* (Hukui 1939; Tuzet & Ormières 1965; Gunderson & Small 1986). The size of the trophozoites in *S. vivax*, however, is the largest known within the genus *Selenidium*. The large size, flattened cell shape and active motility increase the amount of surface area that can interact with the nutrient-rich environment within the lumen of the host intestine. This set of adaptations is remarkably similar to the set of characteristics that has convergently evolved in the individual proglottids of cestode flatworms that inhabit similar environments within their vertebrate hosts. It can be reasonably inferred, therefore, that the cell shape and behaviour of *S. vivax* facilitates nutrient uptake across the cell surface of trophozoites via endocytosis. This is consistent with the possibility that an apical complex (i.e. conoid, rhoptries and micronemes) is absent in trophozoites; this apparatus is present in the trophozoites of many species within *Selenidium* and *Digyalum* and is thought to facilitate the acquisition of nutrients by myzocytosis (Schrével 1968; Dyson et al. 1993, 1994).

However, micropores were not observed over the cell surface in *S. vivax*, which would be an expected mechanism for surface-mediated nutrition. It is highly likely nonetheless that some of the multiple membrane-bound structures found in the cytoplasm (Figure 5D, E) are nutrient-carrying vesicles produced by endocytosis. Vesicles with the same structure and function (so-called "pinocytotic vesicles") have been demonstrated in several archigregarines and intestinal eugregarines (Vivier & Schrével 1964; Vivier 1968; Schrével 1971b; Desportes 1974;

Hoshida & Todd 1996). Like *S. vivax*, the trophozoites of intestinal eugregarines lack an apical complex and have dramatically increased the surface area to volume ratio by folding the cortex into hundreds of longitudinal striations (Vivier 1968; Warner 1968; Vavra & Small 1969; MacMillan 1973; Leander et al. 2003a). Presumably, the epicytic folds help facilitate the surface-mediated uptake of nutrients and gliding motility in eugregarines. Overall, *S. vivax* (together with its flattened relatives) and intestinal eugregarines (e.g. *Lecudina*, *Lankesteria* and *Gregarina*) might represent two independent lineages that have replaced myzocytotic-based feeding using an apical complex with surface-mediated nutrition. Therefore, surface-mediated nutrition seems to be facilitated by significantly increasing cell surface area in at least two different ways: (1) large cell size, cell flattening and active motility in *S. vivax* and (2) cell rigidity and hundreds of epicytic folds in intestinal eugregarines.

The attachment apparatus in *S. vivax*, especially the highly convoluted network of endoplasmic reticulum, is novel. Presumably, the thread-like structures emerging from the linear row of pores along the anterior edge function in the attachment of the parasites to the epithelial cells of the host intestines. It is unclear whether nutrients are absorbed through the pores of the attachment apparatus. The clustering of dense bodies below the attachment apparatus is similar to that found in the trophozoites of other marine gregarines (e.g. Schrével 1968; Dyson et al. 1994; Kuvardina & Simdyanov 2002). Understanding the structural and functional significance of the unidentified linear structure shown in Figure 7D and F will require three-dimensional reconstructions and further analysis.

The structure of the cytoskeleton in *S. vivax* reflects the underlying mechanism behind the active cellular deformations observed in the trophozoites. The trophozoites were capable of twisting, contracting, extending and folding, and generating co-ordinated waves that usually passed from the posterior end to the anterior end of the cell (Figures 1, 2A, B). The parallel bundles of longitudinal microtubules beneath the inner membrane complex appear to be

Figure 3. Scanning (SEMs) and transmission electron micrographs (TEMs) of *Selenidium vivax* showing general characteristics of the trophozoite surface and underlying cytoskeleton. (A, B) SEMs of two trophozoites in a contracted state (upper) and a semi-relaxed state (lower) showing transverse striations over the cell surface (bar = 20 µm). (C–E) SEMs showing the inferred progression in the development of transverse folds. Stretched regions of the trophozoite surface appear smooth or contain transverse rows of tiny longitudinal ridges, arranged in parallel (arrowheads). These transverse rows of parallel ridges develop into continuous transverse folds in contracted regions on the trophozoite cell surface (C, bar = 2.5 µm; D, E, bars = 2 µm). (F) Longitudinal TEM through a trophozoite showing the transverse folds in transverse view, the convoluted plasma membrane (double arrowheads), underlying inner membrane complex and subtending microtubules in longitudinal view (arrowheads) (bar = 0.5 µm). (G) SEM showing longitudinal striations on the trophozoite surface (arrowheads) (bar = 2.5 µm). (H) Transverse TEM showing distinct clusters of microtubules in transverse view (brackets) that correspond to the longitudinal striations shown in (G) (bar = 0.5 µm). (I) High-magnification TEM showing the clustered microtubules in transverse view (arrowheads) (bar = 0.2 µm). (J) High-magnification TEM showing a tangential view of clustered microtubules (arrowheads) (bar = 0.25 µm).

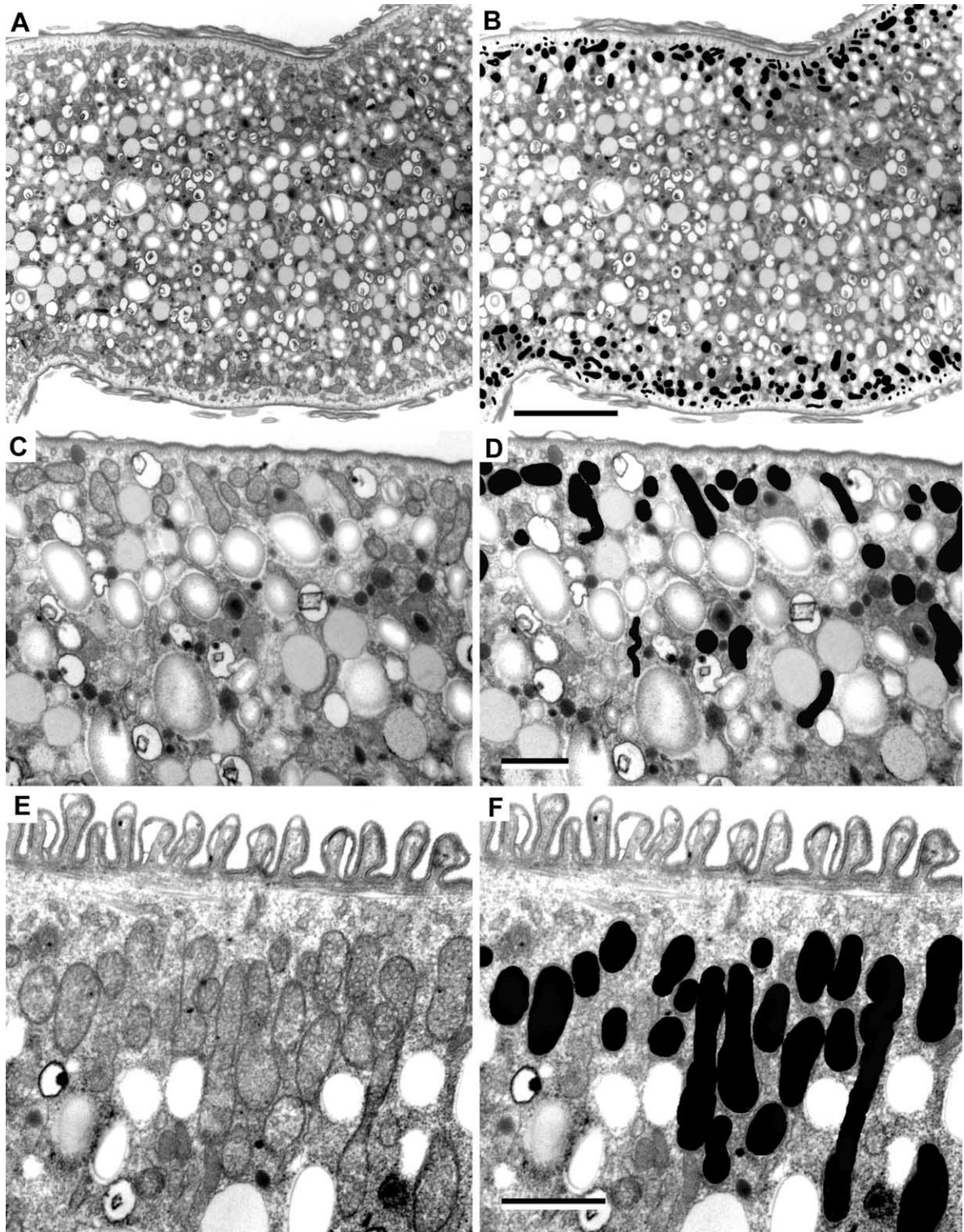


Figure 4. Transmission electron micrographs (TEMs) of *Selenidium vivax* showing the vast, complex cytoplasm of trophozoites and the superficial distribution of mitochondria. (A, B) Identical low-magnification TEMs with the mitochondria highlighted in black in (B) (bar = 4 μm). (C, D) Identical mid-magnification TEMs with the mitochondria highlighted in black in (D) (bar = 1 μm). (E, F) Identical high-magnification TEMs with the mitochondria highlighted in black in (F) (bar = 1 μm).

involved in the production of the forces necessary for cell motility. Studies on the bending movements of flagellar axonemes and oxymonad axostyles have demonstrated that microtubule-associated molecu-

lar motors (MAPs), such as kinesins or dyneins, are responsible for sliding between adjacent microtubules. Although speculative, a similar mechanism acting on pellicular microtubules or adjacent bun-

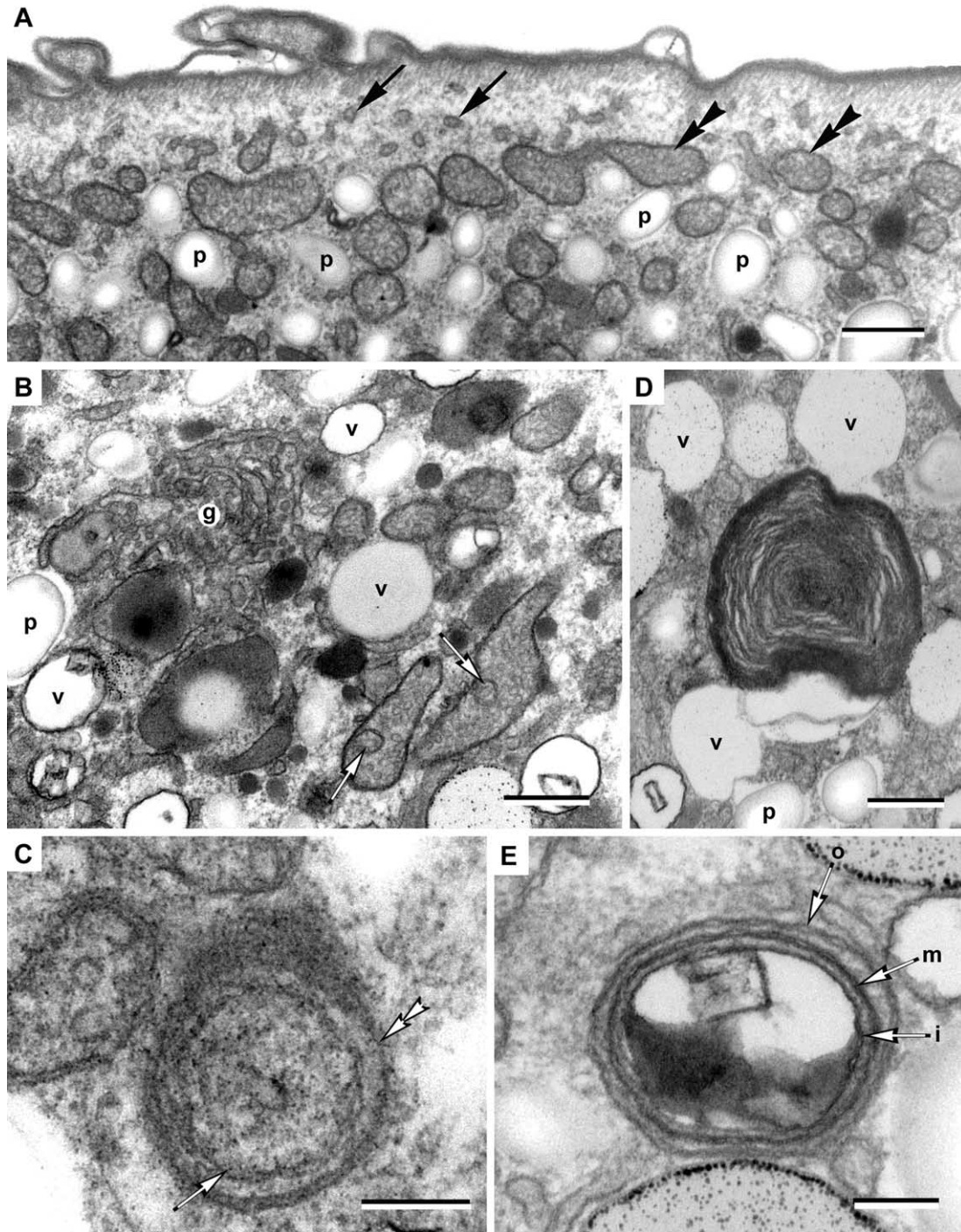


Figure 5. Transmission electron micrographs (TEMs) of *Selenidium vivax* showing the ultrastructure of mitochondria and other multiple membrane-bound organelles. (A) TEM showing mitochondria with well-formed tubular cristae (double arrowheads) and small profiles of mitochondria-like vesicles beneath the cytoskeleton (arrows) (bar = 0.5 μm). (B) TEM showing a Golgi body (g), vesicles (v), paraglycogen granules (p) and mitochondria with ring-shaped inclusions (arrows) (bar = 0.5 μm). (C) High-magnification TEM of a ring-shaped inclusion within a mitochondrion showing a pair of inner membranes (arrow) and a pair of outer membranes (double arrowhead) (bar = 0.2 μm). (D) TEM showing a putative pinocytotic vesicle consisting of a dense accumulation of concentric membranes (bar = 0.5 μm). (E) TEM showing a putative pinocytotic vesicle consisting of three pairs of concentric membranes (arrows; i = inner, m = middle, o = outer). The square-shaped structure within the membranes is probably a fixation artefact (bar = 0.2 μm).

dles of microtubules might be responsible for the cellular deformations observed in *S. vivax*. This putative mechanism would also cause transient longitudinal striations that are consistent with those

observed in *S. vivax*. Moreover, microtubular sliding would help explain the generation of transverse folds on the surfaces of contracted cell regions. If the microtubules (or microtubular bundles) interdigiti-

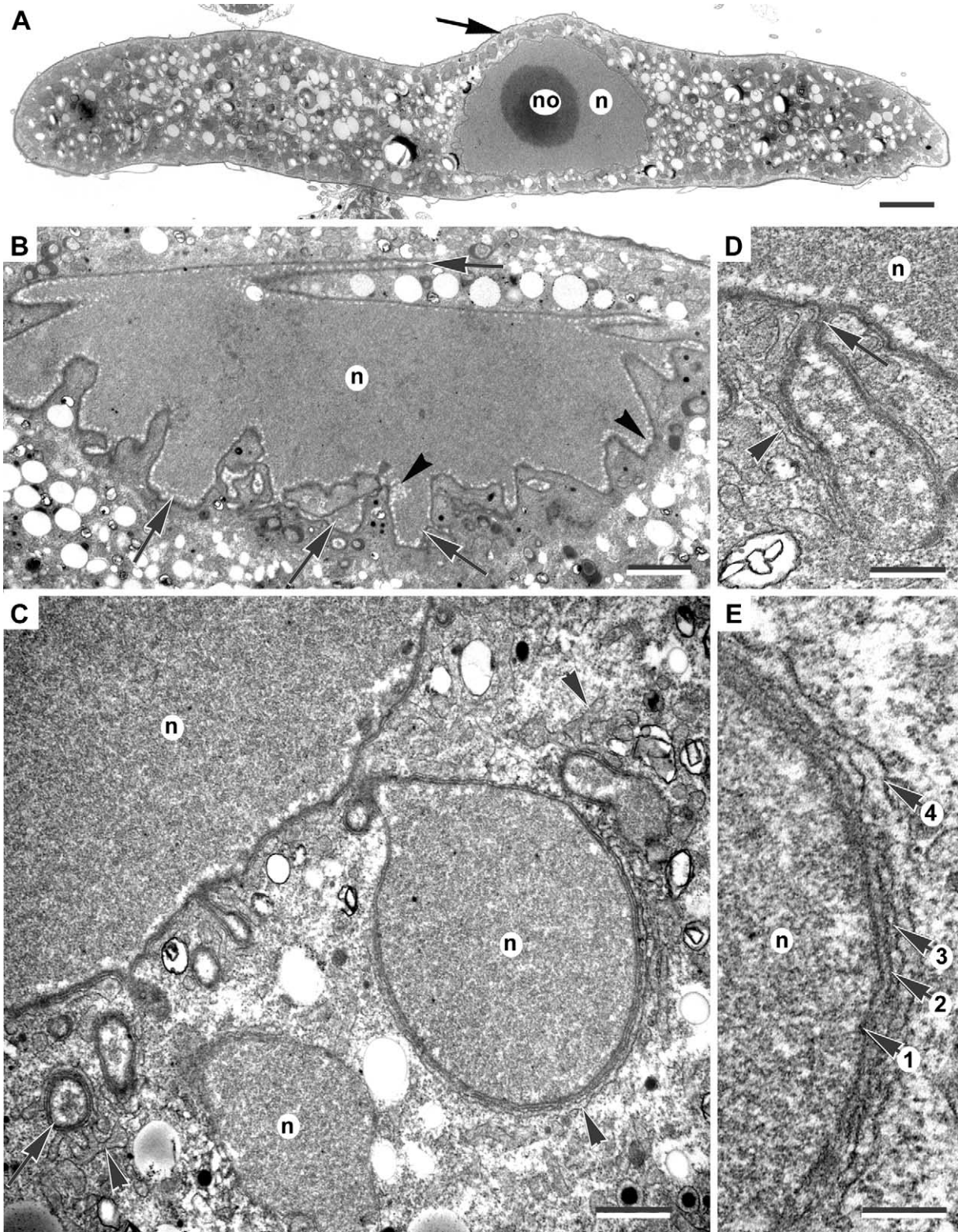


Figure 6. Transmission electron micrographs (TEMs) of *Selenidium vivax* showing the ultrastructure of the nucleus. (A) Transverse TEM through a trophozoite at the level of the nucleus (n) showing the flattened cell shape, the nucleolus (no) and the bulge in the cell created by the large nucleus (arrow) (bar = 4 μm). (B) TEM of a nucleus (n) showing a vesicular layer (arrowheads) positioned beneath the fingers of the convoluted envelope (arrows) (bar = 2 μm). (C) High-magnification TEM showing endoplasmic reticulum (arrowheads) around mitochondria-like organelles (arrow) and vesicle-like projections of the nucleus (n) (bar = 1 μm). (D) TEM showing endoplasmic reticulum (arrowheads) and a bleb emerging from the nucleus (n) by a constricted stalk (arrow) (bar = 0.5 μm). (E) High-magnification TEM showing four membranes (arrow-1, arrow-2, arrow-3, arrow-4) around a nuclear bleb (n). The outer two membranes are interpreted to be endoplasmic reticulum (bar = 0.25 μm).

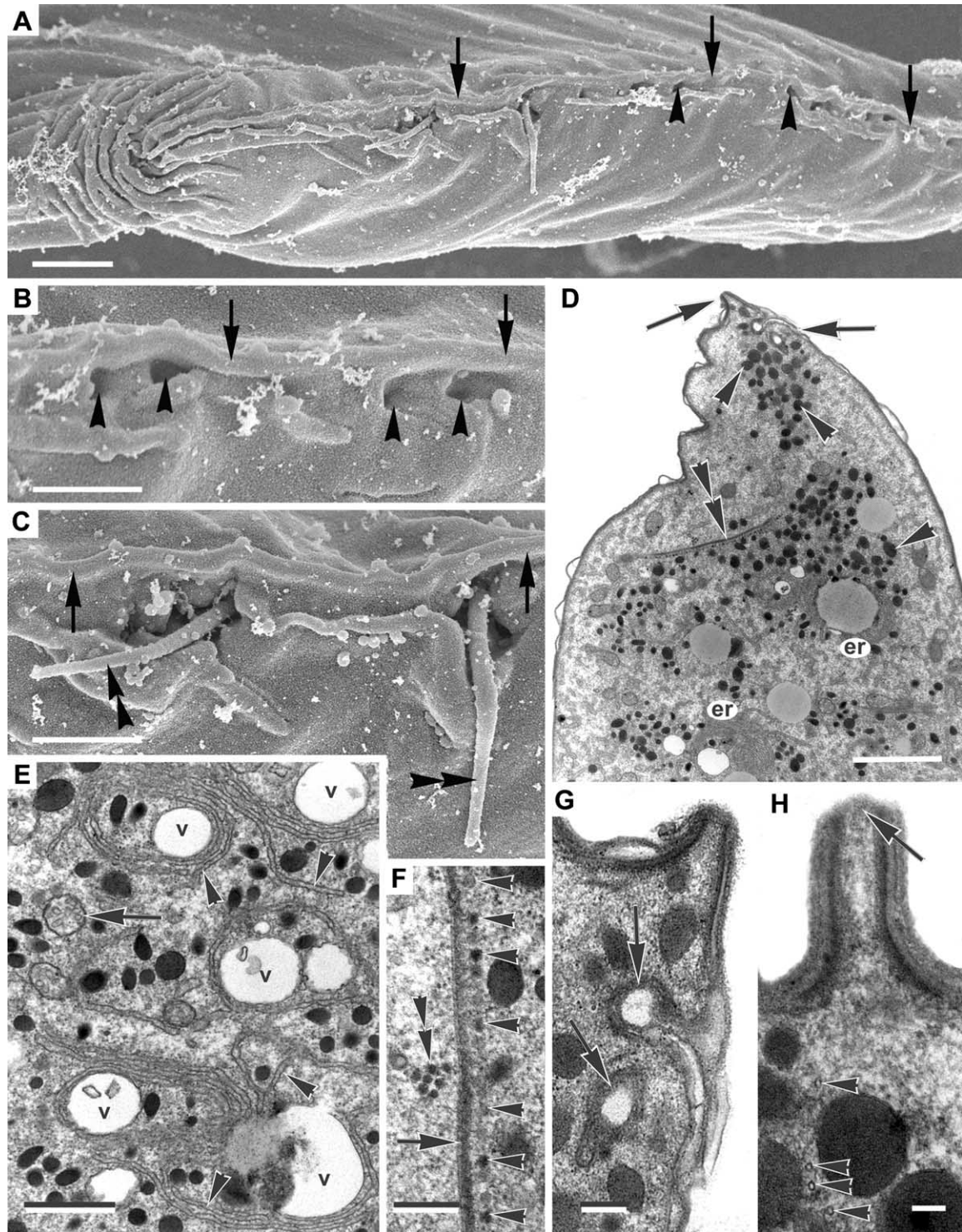


Figure 7. Scanning (SEMs) and transmission electron micrographs (TEMs) of *Selenidium vivax* showing the general characteristics of the trophozoite attachment apparatus (anterior end). (A) Low-magnification SEM showing the anterior edge of a trophozoite consisting of a transverse ridge (arrows) and a linear arrangement of pores (arrowheads) (bar = 2.5 μm). (B, C) High-magnification SEMs showing pores (arrowheads) beneath the transverse ridge (arrows) and thread-shaped structures emerging from the pores (double arrowheads) (bars = 1 μm). (D) Low-magnification TEM of the anterior end showing clusters of dense bodies (arrowheads), endoplasmic reticulum (er), anterior pores (arrows) and an unidentified linear structure (double arrowhead) (bars = 2 μm). (E) Higher magnification TEM showing the distribution of endoplasmic reticulum (arrowheads), vesicles (v), mitochondria (arrow) near the anterior end of trophozoites (bars = 1 μm). (F) High-magnification TEM showing the unidentified linear thread (arrow) shown in (D) with an adjacent row of small electron-dense granules (arrowheads) to the right and a small cluster of seven small electron-dense granules to the left (double arrowhead) (bars = 0.25 μm). (G, H) High-magnification TEMs showing the openings of several pores (arrows) and subtending microtubules (arrowheads) (bars = 0.1 μm).

tate, then the sliding of microtubules towards the middle of the cell would shrink the overall cell length and the overlying inner membrane complex and plasma membrane would need to fold over (wrinkle) in order to compensate. Transverse folds, like those found in *S. vivax*, have been observed in *Digyalum* and other species of *Selenidium* (e.g. Dyson et al. 1993, 1994; Leander et al. 2003a).

The viability of this putative mechanism is enhanced by the fact that a dense layer of mitochondria is positioned superficially in the cells, directly beneath the pellicular microtubules. The presence of highly developed mitochondria suggests that aerobic metabolism is possible within the intestines of the sipunculid host. As generators of ATP, mitochondria provide the chemical energy necessary for MAP activity. Therefore, an intimate association between the mitochondria and pellicular microtubules provides a highly functional configuration for active cellular motility (see also Schrével 1971b). It should also be stressed, however, that dynamic instability of the microtubules might also play a role in the cell motility of *S. vivax*. Nonetheless, a similar MAP-based mechanism has been proposed to explain the undulating and bending movements for other species of *Selenidium* (Schrével 1971b; Stebbings et al. 1974; Mellor & Stebbings 1980).

It remains unclear whether the independent mitochondrial profiles positioned below the pellicular microtubules are linked together within a large reticulum or constitute a population of disconnected organelles. Reticulated mitochondria have been reported in distantly related parasites, such as trypanosomatids (Paulin 1983), and there is some evidence suggesting that a mitochondrial reticulum might be present in some leucidinid gregarines, namely *Cygnicollum lankesteri* (Desportes & Théodoridès 1986). The small mitochondria-like profiles immediately below the pellicular microtubules and the presence of narrow connections between larger mitochondrial profiles is suggestive of an expansive mitochondrial reticulum that completely surrounds the trophozoites in *S. vivax*. Moreover, circular inclusions within some small mitochondrial profiles give the appearance of four membrane-bound organelles (Figure 5C); identical inclusions have been reported in other gregarines (Vivier & Schrével 1966; Schrével 1971b). A more detailed study involving serial sectioning will be required to fully understand mitochondrial structure and organization in this parasite.

The nucleus in the trophozoites of *S. vivax* is enormous (diameter = 20–40 µm in this study; diameter = 23–48 µm in Gunderson & Small 1986), and the large nucleolus and uniform euchromatin are consistent with the nuclear ultrastructure re-

ported in other gregarines and apicomplexans. The convoluted nuclear envelope and nuclear blebs observed in *S. vivax* are uncommon in marine archigregarines, but have been observed in several eugregarines (Desportes & Théodoridès 1969; Baudoin & Ormières 1973; Desportes 1974). The nuclear blebs were of different sizes and were surrounded by a cisterna of endoplasmic reticulum, which gave the appearance of four membrane-bound organelles near the nucleus proper (Figure 6C–E). This general morphology and position within the cell is reminiscent of the apicoplasts (i.e. vestigial photosynthetic organelles surrounded by four membranes) that have been reported in several different apicomplexan lineages (McFadden et al. 1997; Lang-Unnasch et al. 1998; Waller & McFadden 2005). Although apicoplasts have not been definitively demonstrated in gregarines (or *Cryptosporidium*), four membrane-bound organelles of unknown homology and function have been reported in the literature prior to the discovery of apicoplasts (Vivier & Hennere 1965; Schrével 1971b; Porchet-Hennere 1972). Accordingly, it is very difficult to determine from images alone whether the multiple membrane-bound organelles in the earlier literature represent apicoplasts or other cellular inclusions such as the nuclear blebs or pinocytotic vesicles reported here.

Acknowledgements

I wish to thank two anonymous reviewers for their attentive and constructive feedback. This work was supported by grants to B.S.L. from the National Science and Engineering Research Council of Canada (NSERC 283091-04) and the Canadian Institute for Advanced Research, Program in Evolutionary Biology.

References

- Baudoin J, Ormières R. 1973. Sur quelques particularités de l'ultrastructure de *Didymophyes chaudefouri* Ormières, Eugregarine, Didymophyidae. Comptes Rendus Hebdomadaires des Séances de l'Académie des Sciences. Paris (Series D) 277:73–5.
- Cavalier-Smith T, Chao EE. 2004. Protalveolate phylogeny and systematics and the origins of Sporozoa and dinoflagellates (phylum Myzozoa nom. nov.). European Journal of Protistology 40:185–212.
- Cox FEG. 1994. The evolutionary expansion of the sporozoa. International Journal for Parasitology 24:1301–16.
- Desportes I. 1974. Ultrastructure et evolution nucléaire des trophozoïtes d'une grégarine d'éphéméroptère: *Enterocystis fungoides* M. Codreanu. Journal of Protozoology 21:83–94.
- Desportes I, Théodoridès J. 1969. Ultrastructure de la grégarine *Callynthrochlamys phronimae* Frenzel; étude comparée de son Noyau avec celui de *Thalicola salpae* (Frenzel) (Eugregarina). Journal of Protozoology 16:449–60.
- Desportes I, Théodoridès J. 1986. *Cygnicollum lankesteri* n. sp., grégarine (Apicomplexa, Lecudinidae) parasite des annélides

- polychètes *Laetmonice hystrix* et *L. producta*; particularités de l'appareil de fixation et implications taxonomiques. *Protistologica* 22:47–60.
- Dyson J, Grahame J, Evennett PJ. 1993. The mucron of the gregarine *Digyalum oweni* (Protozoa, Apicomplexa), parasitic in *Littorina* species (Mollusca, Gastropoda). *Journal of Natural History* 27:557–64.
- Dyson J, Grahame J, Evennett PJ. 1994. The apical complex of the gregarine *Digyalum oweni* (Protozoa, Apicomplexa). *Journal of Natural History* 28:1–7.
- Grassé P-P. 1953. Classe des grégariomorphes (Gregarinomorpha n. nov.; Gregarinae Haeckel, 1866; gregarinidea Lankester, 1885; grégariines des auteurs). In: Grassé P-P, editor. *Traité de Zoologie*. Paris: Masson. p 590–690.
- Gunderson J, Small EB. 1986. *Selenidium vivax* n. sp. (Protozoa, Apicomplexa) from the sipunculid *Phascolosoma agassizii* Keferstein, 1867. *Journal of Parasitology* 72:107–10.
- Hoshida K, Todd KS. 1996. The fine structure of cell surface and hari-like projections of *Filipodium ozaki* Hukui 1939 gamonts. *Acta Protozoologica* 35:309–15.
- Hukui T. 1939. On the gregarines from *Siphonosoma cumanense* (Keferstein). *Journal of Science of the Hiroshima University* (ser. B, div. 1) 7:1–23.
- Kuvarina ON, Leander BS, Aleshin VV, Mylnikov AP, Keeling PJ, Simdyanov TG. 2002. The phylogeny of colpodellids (Eukaryota, Alveolata) using small subunit rRNA genes suggests they are the free-living ancestors of apicomplexans. *Journal of Eukaryotic Microbiology* 49:498–504.
- Kuvarina ON, Simdyanov TG. 2002. Fine structure of syzygy in *Selenidium pennatum* (Sporozoa, Archigregarinida). *Protistology* 2:169–77.
- Lang-Unnasch N, Reith ME, Munholland J, Barta JR. 1998. Plastids are widespread and ancient in parasites of the phylum Apicomplexa. *International Journal for Parasitology* 28:1743–54.
- Leander BS, Harper JT, Keeling PJ. 2003a. Molecular phylogeny and surface morphology of marine aseptate gregarines (Apicomplexa): *Lecudina* and *Selenidium*. *Journal of Parasitology* 89:1191–205.
- Leander BS, Keeling PJ. 2003. Morphostasis in alveolate evolution. *Trends in Ecology and Evolution* 18:395–402.
- Leander BS, Kuvarina ON, Aleshin VV, Mylnikov AP, Keeling PJ. 2003b. Molecular phylogeny and surface morphology of *Colpodella edax* (Alveolata): insights into the phagotrophic ancestry of apicomplexans. *Journal of Eukaryotic Microbiology* 50:334–40.
- Leander BS, Lloyd SAJ, Marshall W, Landers SC. 2006. Phylogeny of marine gregarines (Apicomplexa) – *Pterospora*, *Lithocystis* and *Lankesteria* – and the origin(s) of coelomic parasitism. *Protist* 157:45–60.
- Levine ND. 1971. Taxonomy of the Archigregarinorida and Selenidiidae (Protozoa, Apicomplexa). *Journal of Protozoology* 18:704–17.
- MacMillan WG. 1973. Conformational changes in the cortical region during peristaltic movements of a gregarine trophozoite. *Journal of Protozoology* 20:267–74.
- McFadden GI, Waller RF, Reith ME, Lang-Unnasch N. 1997. Plastids in apicomplexan parasites. In: Bhattacharya D, editor. *Plant Systematics and Evolution*. Berlin: Springer. p 261–87.
- Mellor JS, Stebbings H. 1980. Microtubules and the propagation of bending waves by the archigregarine, *Selenidium fallax*. *Journal of Experimental Biology* 87:149–61.
- Mylnikov AP. 1991. The ultrastructure and biology of some representatives of order Spiromonadida (Protozoa). *Zoologicheskij Zhurnal* 70:5–15.
- Mylnikov AP. 2000. The new marine carnivorous flagellate *Colpodella pontica* (Colpodellida, Protozoa). *Zoologicheskij Zhurnal* 79:261–6.
- Paulin JJ. 1983. Conformation of a single mitochondrion in the trypomastigote stage of *Trypanosoma cruzi*. *Journal of Parasitology* 69:242–4.
- Porchet-Hennere E. 1972. Observations en microscopie photographique et électronique sur la sporogenèse de *Dehornia sthenelais* (n. gen., sp. n.), sporozoaire parasite de l'annelide polychète *Sthenelais boa* (Aphroditides). *Protistologica* 8:245–55.
- Ray HN. 1930. Studies on some protozoa in polychaete worms. I. Gregarines of the genus *Selenidium*. *Parasitology* 22:370–400.
- Schrével J. 1968. L'ultrastructure de la région antérieure de la gregarine *Selenidium* et son intérêt pour l'étude de la nutrition chez les sporozoaires. *Journal of Microscopie* 7:391–410.
- Schrével J. 1970. Contribution à l'étude des Selenidiidae parasites d'annelides polychètes. I. Cycles biologiques. *Protistologica* 6:389–426.
- Schrével J. 1971a. Observations biologique et ultrastructurales sur les Selenidiidae et leurs conséquences sur la systématique des grégariomorphes. *Journal of Protozoology* 18:448–70.
- Schrével J. 1971b. Contribution à l'étude des Selenidiidae parasites d'annelides polychètes. II. Ultrastructure de quelques trophozoites. *Protistologica* 7:101–30.
- Simpson AGB, Patterson DJ. 1996. Ultrastructure and identification of the predatory flagellate *Colpodella pugnax* Cienkowski (Apicomplexa) with a description of *Colpodella turpis* n. sp. and a review of the genus. *Systematic Parasitology* 33:187–98.
- Stebbins H, Boe GS, Garlick PR. 1974. Microtubules and movement in the archigregarine, *Selenidium fallax*. *Cell and Tissue Research* 148:331–45.
- Théodoridès J. 1984. The phylogeny of the Gregarina. *Origin of Life* 13:339–42.
- Tuzet O, Ormières R. 1965. Sur quelques Gregarines parasites de *Phascolion* et *Aspidosiphon* (Sipunculien). *Protistologica* 1:43–8.
- Vavra J, Small EB. 1969. Scanning electron microscopy of gregarines (Protozoa, Sporozoa) and its contribution to the theory of gregarine movement. *Journal of Protozoology* 16:745–57.
- Vivier E. 1968. L'organisation ultrastructurale corticale de la gregarine *Lecudina pellucida*: ses rapports avec l'alimentation et la locomotion. *Journal of Protozoology* 15:230–46.
- Vivier E, Desportes I. 1990. Phylum Apicomplexa. In: Margulis L, Corliss JO, Melkonian M, Chapman DJ, editors. *The Handbook of Protozoology*. Boston: Jones and Bartlett. p 549–73.
- Vivier E, Hennere E. 1965. Ultrastructure des stades végétatifs de la coccidie *Coelotropha durchoni*. *Protistologica* 1:89–104.
- Vivier E, Schrével J. 1964. Étude, au microscope électronique, d'une gregarine du genre *Selenidium*, parasite de *Sabellaria alveolata* L. *Journal of Microscopie* 3:651–70.
- Vivier E, Schrével J. 1966. Les ultrastructures cytoplasmiques de *Selenidium hollandei*, n. sp. gregarine parasite de *Sabellaria alveolata* L. *Journal of Microscopie* 5:213–28.
- Waller RF, McFadden GI. 2005. The apicoplast: a review of the derived plastid of apicomplexan parasites. *Current Issues in Molecular Biology* 7:57–80.
- Warner FD. 1968. The fine structure of *Rhynchocystis pilosa* (Sporozoa, Eugregarinida). *Journal of Protozoology* 15:59–73.